

1
2
3
4
5
6
7 **A simple graphite-based support material**
8
9
10 **for robocasting of ceramic parts**
11
12
13
14
15
16

17 Francisco J. Martínez-Vázquez*, Antonia Pajares, Pedro Miranda
18
19
20
21

22
23 Departamento de Ingeniería Mecánica, Energética y de los Materiales, Universidad
24
25 de Extremadura. Avda de Elvas s/n. 06006 Badajoz, Spain
26
27
28
29
30
31

32
33 * Corresponding author.
34

35 F.J. Martínez-Vázquez's contact details:
36

37
38 Email: fjmartinezv@unex.es
39

40
41 Phone: +34 924 28 92 52
42

43
44 Fax: +34 924 28 96 01
45

46
47 Escuela de Ingenierías Industriales
48

49
50 Avda de Elvas s/n. 06006 Badajoz, Spain
51
52
53
54
55
56
57
58
59
60
61
62
63
64
65

1
2
3
4
5
6
7
8
9
10
11
12
13
14
15
16
17
18
19
20
21
22
23
24
25
26
27
28
29
30
31
32
33
34
35
36
37
38
39
40
41
42
43
44
45
46
47
48
49
50
51
52
53
54
55
56
57
58
59
60
61
62
63
64
65

Abstract

A simple graphite-based recipe is proposed for use as secondary fugitive ink for robocasting. The ink exhibits excellent rheological performance and physico-chemical compatibility with other ceramic inks and can be completely burned-out by a heat treatment at 800 °C for 2h. The simplicity of the preparation process, together with its low cost, make it an optimal choice for this task. The development of such an ink will greatly facilitate the manufacture of complex ceramic parts requiring the use of a support structure during assembly by direct ink writing.

Keywords

Robocasting; direct ink writing; fugitive ink; support material; graphite

Introduction

The fabrication of complex three dimensional parts is crucial for a wide variety of technological applications in multiple industries such as aerospace, automotive, or biomedical devices, to name a few. Over the last decades, bottom-up strategies for the fabrication of such parts, globally referred to as additive manufacturing (AM)—or, more colloquially, 3D printing —techniques, have gained increased attention [1]. Among the wide variety of AM technologies (stereolithography, selective laser sintering, etc.), direct-write techniques offer the greater versatility and a particular suitability for the fabrication of ceramic parts [2]. In particular, robocasting, also referred as direct ink writing [3], has already been successfully used for the commercialization of certain ceramic products [4] and is receiving increasing attention by ceramic research groups all over the world [4–8]. This technique comprises the use of inks with controlled rheological behaviour capable of retaining their shape during the layerwise extrusion-based assembly process.

The self-supporting capacity of the robocasting inks allows the fabrication of porous structures and some very complex shapes without requiring the use of molds or sacrificial support materials. However, as also occurs in other AM techniques, under certain circumstances (e.g. when spanning large gaps or creating large overhanging features) it is unavoidable to use a secondary support structure to warrantee the proper assembly of a specific design. In these cases, algorithms for calculating the

1
2
3
4 support structure pattern and a system allowing for the alternate printing of the two
5
6 materials now comprising the model are needed. And, most importantly, a suitable
7
8 secondary ink of a fugitive material is required.
9
10

11 The ink of support material must, obviously, meet the typical requirements for a
12
13 robocasting ink, namely: it must maintain its shape even under the load of overlaying
14
15 layers and, under higher shear stresses, be able to flow through fine deposition
16
17 nozzles without clogging. Additionally, this ink must be chemically compatible with the
18
19 colloidal ink of the main material, and easily removable in the post-processing steps,
20
21 leaving no byproducts after decomposition. A suitable method for the elimination of
22
23 the support structure would be to burn it out along with any binder present in the
24
25 deposited inks. In the case of robocast ceramics parts, the selection of a suitable
26
27 material for this fugitive ink is facilitated by the high sintering temperatures required
28
29 for consolidation of the printed structures. However, the intrinsic fragility of ceramics
30
31 and the extreme weakness of the green structure impose the additional requirement
32
33 that such secondary ink must exhibit a degree of shrinkage similar to that of the main
34
35 one. This is necessary to avoid the generation of (micro)cracks during the drying
36
37 process, which would likely propagate during sintering. Finally, since these inks are
38
39 intended to be removed, it is preferable to formulate them from inexpensive materials
40
41 and they should be easy to prepare. Therefore, simple recipes, avoiding the use of too
42
43 many additives, should be sought in order to reduce the preparation time.
44
45
46
47
48
49
50
51
52
53
54

55 The literature on the development of such support inks is still scarce. Wax-based
56
57 inks have been reported to be suitable as fugitive support materials for building
58
59
60
61
62
63
64
65

1
2
3
4 microvascular networks and other polymer-based structures [9,10]. However, this is
5
6 not an ideal solution for the fabrication of ceramic parts by robocasting since
7
8 elimination of such supports involves melting, and the forces associated to this
9
10 process may affect the structural integrity of the weak ceramic green part. Also, this
11
12 and other polymer-based supports may exhibit significantly different levels of
13
14 contraction compared to the main ceramic-based ink during drying, which might also
15
16 produce cracking in the ceramic green body. A more suitable solution has been
17
18 proposed by Smay and col. [11] consisting on the use of a concentrated aqueous gel
19
20 of carbon black as a combustible support material [12]. **Although the feasibility of such**
21
22 **procedure was evidenced in those work by optical images, the details of the**
23
24 **preparation and debinding procedure for such ink has not yet been published, to the**
25
26 **best of our knowledge. Consequently, it is not possible for other authors to replicate**
27
28 **that route. For that reason, this work seeks to provide the first detailed recipe for a**
29
30 **fugitive carbon-based ink for robocasting, as a solution for building complex ceramic**
31
32 **parts that require a support material, and to give details on the ink rheological**
33
34 **properties and the appropriate debinding procedure.**
35
36
37
38
39
40
41
42
43
44

47 **Experimental method**

48 *Materials and ink preparation*

49
50 Aqueous suspensions of graphite powder (282863 Sigma Aldrich, particle size
51
52 **<20 μm , as provided by supplier**) were prepared using carboxymethyl cellulose (CMC)
53
54 (CMC-35, Mw=35,000, Lamberti Iberia S.A.U., Castellón, Spain) as the single
55
56
57
58
59
60
61
62
63
64
65

1
2
3
4 multifunctional (dispersant, binder...) additive [4]. An aqueous solution (4 wt.%) of
5
6 CMC was prepared and then graphite powder was added to create a suspension.
7
8 Solid (graphite) content was varied from 35 to 50 wt.% in order to determine the
9
10 optimal composition of the ink. The powder was added in a single batch and,
11
12 subsequently, the ink was homogenized for 7 min at 700 revolutions per minute in a
13
14 planetary mixer (ARE 250, Thinky Corp., Japan).
15
16
17
18
19

20 The rheological properties of the colloidal inks prepared were evaluated using a
21
22 rheometer (DHR-2, TA Instruments) and a plate-plate geometry (40 mm diameter,
23
24 550 μm gap). Storage modulus was measured in oscillatory mode at 10 Hz, within the
25
26 oscillatory stress range of 0.1–100 Pa. This enabled also the estimation of the ink yield
27
28 stress as the critical oscillatory stress at which the initially linear response (linear
29
30 viscoelastic regime) ends [13].
31
32
33
34

35 In order to demonstrate the suitability of the optimized graphite ink as fugitive
36
37 support for brittle ceramic parts, an alumina (SPA-0.5, Ceralox, Sasol North America
38
39 Inc., USA; particle size distribution: D90 = 0.8 μm , D50 = 0.4 μm , D10 = 0.2 μm , as
40
41 provided by supplier) ink (45 vol.%) was prepared. Briefly, a concentrated stable
42
43 suspension of the alumina powder in distilled water was prepared by using Darvan® C
44
45 (R.T. Vanderbilt, Norwalk, CT) as a dispersant (2.5 wt.% of dispersant relative to the
46
47 weight of alumina). Then hydroxypropyl methylcellulose (Methocel F4M, Dow
48
49 Chemical Company, Midland, MI) was added to the mixture to increase viscosity and
50
51 the ink was finally gellified by adding 4 vol.% of polyethylenimine (PEI), relative to the
52
53 total liquid content.
54
55
56
57
58
59
60
61
62
63
64
65

1
2
3
4 *Robocasting, thermal treatment and characterization*
5

6
7 The developed inks were transferred into separate dispensable cartridges and,
8
9 after removing any trapped bubbles **by repeated vigorous tapping**, placed in a
10 computer-controlled robocasting system (Aerotech A3200, supplied by 3D Inks,
11 Stillwater, OK, USA). The inks were sequentially extruded through conical nozzles ($d \geq$
12 250 μm) in order to fabricate **a sphere, as a good example of** a three-dimensional
13 structure requiring the use of supports. The 3D model for this part and its support
14 structure was generated using an appropriate control software (Robocad 4.2, 3D Inks,
15 Stillwater, OK, USA). Deposition was carried out in air, **rather than within an oil bath,**
16 **which seems to** provide better mechanical performance in the case of solid ceramic
17 parts [15]. After assembly, the 3D bicomponent structure was dried out for 24 h at
18 room temperature. **No humidity control was required to avoid crack formation for the**
19 **materials tested in this work, which does not mean such control may not be required**
20 **in other systems or parts.**
21
22
23
24
25
26
27
28
29
30
31
32
33
34
35
36
37
38
39

40 Thermogravimetric analysis (TGA) was carried out (heating ramp of 10 $^{\circ}\text{C min}^{-1}$)
41 **as a first step in determining** the optimal thermal treatment to remove the fugitive
42 material. The results of the **graphite ink** TGA were corroborated by putting a bulk
43 graphite parallelepiped structure of 7×10×20 mm in a tubular furnace and optically
44 evaluating the volatilization process. For this purpose, photographs of this structure
45 were taken during a heating ramp (10 $^{\circ}\text{C min}^{-1}$) at different temperatures through a
46 suitable observation window, and the variation in its cross-sectional area was
47 determined.
48
49
50
51
52
53
54
55
56
57
58
59
60
61
62
63
64
65

1
2
3
4 The bicomponent 3D assembly was subsequently thermally treated in air to
5
6 remove the graphite and all ink binders using a heating rate of $3\text{ }^{\circ}\text{C min}^{-1}$ up to the
7
8 optimal temperature, where the part was kept for 2 h. Later, a heating ramp of
9
10 $3\text{ }^{\circ}\text{C min}^{-1}$ was set up to $1550\text{ }^{\circ}\text{C}$ where sample was hold for 2 h to ensure the sintering
11
12 of the alumina structure.
13
14

15
16
17 The microstructure of the support material struts in as-dried state was analyzed
18
19 through Scanning Electron Microscopy (SEM) observations (S-3600N, Hitachi,
20
21 Japan), while the quality of the fabricated part was assessed by optical means.
22
23

24
25 Three-point bending tests were performed on graphite filaments (extruded
26
27 through nozzles with a diameter of $584\text{ }\mu\text{m}$) using a universal testing machine (AG-
28
29 IS10kN, Shimadzu Corp., Kyoto, Japan). Tests were performed in air, at a constant
30
31 cross-head speed of 0.6 mm min^{-1} . The flexural strength of the filaments was
32
33 estimated as the maximum stress applied in each test. A total of 25 samples were
34
35 tested in order to obtain statistically reliable values. Weibull statistics were used for
36
37 the analysis of the resulting strength data.
38
39
40
41
42
43
44

45 **Results and Discussion**

46
47 As a first step, ink performance was evaluated in terms of extrudability. Inks rich in
48
49 graphite (50 wt. % and over) were difficult to extrude through deposition nozzles with a
50
51 diameter of $250\text{ }\mu\text{m}$ and, thus, were rejected. Inks with lower graphite contents exhibited
52
53 excellent flowing behavior, attesting to the aptness of the binder selected in this study.
54
55 Due to the apolar nature of graphite, CMC becomes a more appropriate choice over other
56
57
58
59
60
61
62
63
64
65

1
2
3
4 options like ionic polyelectrolites. The lower charge of this multifunctional binder facilitates
5
6
7 greater adsorption [16] onto the graphite surface. This, in turn, enhances its effectiveness
8
9
10 as dispersant—enabling the incorporation of a great amount of powder into the
11
12 suspension—as well as a network forming (i.e. gelling) agent.
13

14
15 Rheological measurements provide a quantification of the inks mechanical
16
17 properties, enabling the identification of the optimal ink composition. Figure 1a shows the
18
19 shear elastic (storage) modulus, G' , versus oscillation stress amplitude, τ , for graphite
20
21 suspensions with solid contents of 35 wt.%, 40 wt.% and 47 wt.%. For all of them, linear
22
23 viscoelastic plateaus are noticeable, preceding an accentuated fall of G' at a given
24
25 oscillatory yield stress, τ_y , when the gel network starts to collapse. Although the plateau
26
27 is less defined for more concentrated slurries, with G' decreasing more significantly with
28
29 the shear stress, ink modulus monotonously increased with graphite content at any given
30
31 shear stress, and the yield stress was also greater in the more concentrated inks. This is
32
33 more clearly appreciated in Figure 1b which shows the evolution of the static elastic
34
35 modulus G'_0 (estimated as the value of the storage modulus G' at $\tau = 0.1$ Pa) and the
36
37 oscillatory yield stress τ_y with the graphite content. A dramatic increase of both properties
38
39 is observed with increasing graphite content. The ink stiffness increased by almost 4
40
41 orders of magnitude from $3.8 \cdot 10^3$ Pa at 35 wt.% to $1.3 \cdot 10^7$ Pa at 47 wt.%, and similarly τ_y
42
43 increased by a factor of 6.3, from 0.91 Pa to 5.74 Pa. Since maximum values from both
44
45 magnitudes are desirable features for robocasting inks—as they represent the ability of
46
47 the ink to sustain load and retain shape—it is evident that the optimal ink is that with
48
49
50
51
52
53
54
55
56
57
58
59
60
61
62
63
64
65

1
2
3
4 47 wt.% of graphite. This ink exhibited the highest G' and τ_y values while still maintaining
5
6
7 excellent extrudability.
8

9
10 Those values are indeed high enough to warranty the ability of this ink to sustain
11 the load of any overlayers even when deposited in the form of an open porous support
12 scaffold. The structural quality of the ink can be assessed also on the SEM micrograph
13
14 of Figure 2, showing one such a porous robocast structure made from the graphite ink, in
15
16 as-dried condition. The rods show a good circular shape in the transversal section of the
17
18 rods—i.e. they are not deformed into an elliptical shape by the weight of the overlaying
19
20 material— and they remain straight, without sagging into a catenary shape, when
21
22 spanning underlying gaps. Regarding the microstructural features, the graphite platelets
23
24 have been evidently aligned parallel to the rod axis during the extrusion of the ink. As a
25
26 consequence, the microporosity, which is nonetheless high as correspond to a green
27
28 body, is somewhat lower close to the rod surface. This is deemed to be beneficial to the
29
30 strength and mechanical integrity of the support structures, especially, after drying. In
31
32 fact, the flexural strength of the green graphite filaments—estimated as the central value
33
34 of the corresponding Weibull distribution— was measured to be 1.04 ± 0.04 MPa, which
35
36 is remarkably high for unsintered struts.
37
38
39
40
41
42
43
44
45
46

47
48 Concerning the optimal temperature for burning out the graphite ink, Figure 3
49 shows both the TGA data (left Y axis) and the evolution of the cross sectional area
50 (normalized to its initial value, right Y axis) for a given graphite scaffold with temperature.
51
52 In spite of the fact that the structure was dried for 24 h at room temperature before
53
54 initiating the thermal treatment, the first weight (and area) loss (200-500 °C) is due to the
55
56
57
58
59
60
61
62
63
64
65

1
2
3
4 evaporation of residual, adsorbed water, plus the elimination of the carboxymethyl
5
6 cellulose (autoignition temperature is 370 °C, according to MSDS). Thereafter, a
7
8 significant increase in material loss is produced upon the onset of graphite oxidation
9
10 (~ 500 °C) into gaseous species, mainly CO₂. It can be seen that both the weight and the
11
12 area loss rates reached a maximum value at around 600 °C. However, an incomplete
13
14 oxidation takes place at times up to 2h at this temperature producing local discoloration
15
16 in the adjacent ceramic part during the sintering stage. To avoid this undesired interaction,
17
18 a somewhat higher temperature of 800 °C ensured the complete elimination of the
19
20 graphite structures in 2 h or less, without discoloration of adjacent ceramic parts. Thus, a
21
22 heat treatment at 800 °C for 2h was selected as optimal for the removal of the graphite
23
24 supports fabricated using the ink composition proposed in this work. Optimal heating
25
26 ramp will depend of the robocasting ink composition used for the ceramic part.
27
28
29
30
31
32
33
34

35 Figure 4 illustrates the fabrication of a sphere using the developed support inks.
36
37 Figure 4a shows the as-dried alumina green part fabricated using the ink with 47 wt.%
38
39 graphite content as support material. There is no evidence of cracking in the brittle
40
41 alumina sample due to shrinkage mismatch. Measured linear shrinkage during drying was
42
43 low for both materials: 3.7 ± 0.8 % for the alumina part and 4 ± 1 % for the graphite
44
45 support. If the ceramic part had a larger shrinkage, typical for example in inks involving
46
47 ceramic nanopowders—e.g. a 26 vol.% hydroxyapatite ink fabricated by our group from
48
49 nano-sized powders (Captal R, Plasma Biotel Ltd., UK) has a shrinkage of 10.1 ± 0.7 %—
50
51 , it is possible to adjust the shrinkage of the graphite ink by reducing also its solid content
52
53 from the optimal value indicated in this work. In that case, in order to preserve the
54
55
56
57
58
59
60
61
62
63
64
65

1
2
3
4 rheological properties of the fugitive ink it is necessary to increase the CMC content. For
5
6
7 example, an ink with 35 wt.% of graphite and suitable printability was fabricated by
8
9
10 increasing the CMC content from 4 wt.% to 10 wt.%. Such an ink exhibited a shrinkage
11
12 of 9 ± 1 %, which matches within the errors the shrinkage of the aforementioned nano-
13
14 hydroxylapatite ink. Nonetheless, the authors would like to point out that a high level of
15
16 shrinkage in both the ceramic part and its support structure during drying should be
17
18 avoided whenever possible—by maximizing the solid content in the robocasting inks—,
19
20 not only to minimize the possibility of cracking during drying, but also to increase shape
21
22 retention. In any case, it is evident that the proposed graphite ink can indeed be used to
23
24
25 match the shrinkage of any ceramic part.
26
27
28

29
30 Moreover, as evidenced in Fig. 4b, showing the same part after the burn-out and
31
32 sintering heat treatment, the graphite ink was completely removed after the heat
33
34 treatment, leaving either no signal of discoloration or deformation of the ceramic part.
35
36 Thus, the graphite ink was demonstrated to be an adequate candidate as support material
37
38 for complex 3D models that require the use of such scaffolds during assembly.
39
40
41
42
43

44 **Conclusion**

45
46
47
48
49
50 The graphite ink proposed in this work fulfils all the necessary requirements for
51
52 use as secondary fugitive ink for robocasting of ceramic parts. The excellent rheological
53
54 performance and the simplicity of the preparation process, the possibility of matching its
55
56 shrinkage to that of the primary ink, together with its low cost and physico-chemical
57
58
59
60
61
62
63
64
65

1
2
3
4 compatibility with other ceramic inks make it an optimal choice for this task. The
5
6 development of such a simple support ink will greatly facilitate the manufacture of
7
8 complex ceramic parts by direct ink writing.
9
10
11
12
13
14
15
16
17
18
19
20
21

22 **Acknowledgements**

23
24 This work was supported by the Ministerio de Economía y Competitividad [grant
25
26 MAT2015-64670-R (MINECO/FEDER)], the Junta de Extremadura [grant IB16094] and
27
28 the Fondo Europeo de Desarrollo Regional (FEDER).
29
30
31
32
33
34
35
36
37
38
39
40
41
42
43
44
45
46

47 **References**

- 48
49
50 [1] K. V. Wong, A. Hernandez, A Review of Additive Manufacturing, ISRN Mech.
51
52 Eng. 2012 (2012) 1–10. doi:10.5402/2012/208760.
53
54
55 [2] J.A. Lewis, G.M. Gratson, Direct writing in three dimensions, Mater. Today. 7
56
57 (2004) 32–39. doi:10.1016/S1369-7021(04)00344-X.
58
59
60
61
62
63
64
65

- 1
2
3
4 [3] F.J. Martínez-Vázquez, F.H. Perera, P. Miranda, A. Pajares, F. Guiberteau,
5
6 Improving the compressive strength of bioceramic robocast scaffolds by polymer
7
8 infiltration., *Acta Biomater.* 6 (2010) 4361–8. doi:10.1016/j.actbio.2010.05.024.
9
10
11 [4] S. Eqtesadi, A. Motealleh, P. Miranda, A. Lemos, A. Rebelo, J.M.F. Ferreira, A
12
13 simple recipe for direct writing complex 45S5 Bioglass® 3D scaffolds, *Mater. Lett.*
14
15 93 (2013) 68–71. doi:10.1016/j.matlet.2012.11.043.
16
17
18 [5] E. García-Tuñón, S. Barg, J. Franco, R. Bell, S. Eslava, E. D’Elia, et al., Printing
19
20 in Three Dimensions with Graphene, *Adv. Mater.* 27 (2015) 1688–1693.
21
22 doi:10.1002/adma.201405046.
23
24
25 [6] K. Cai, B. Román-Manso, J.E. Smay, J. Zhou, M.I. Osendi, M. Belmonte, et al.,
26
27 Geometrically Complex Silicon Carbide Structures Fabricated by Robocasting, *J.*
28
29 *Am. Ceram. Soc.* 95 (2012) 2660–2666. doi:10.1111/j.1551-2916.2012.05276.x.
30
31
32 [7] M.C. Matesanz, J. Linares, M. Oñaderra, M.J. Feito, F.J. Martínez-Vázquez, S.
33
34 Sánchez-Salcedo, et al., Response of osteoblasts and preosteoblasts to calcium
35
36 deficient and Si substituted hydroxyapatites treated at different temperatures.,
37
38 *Colloids Surf. B. Biointerfaces.* 133 (2015) 304–13.
39
40
41 doi:10.1016/j.colsurfb.2015.06.014.
42
43
44 [8] A. Zocca, G. Franchin, H. Elsayed, E. Gioffredi, E. Bernardo, P. Colombo, Direct
45
46 Ink Writing of a Pre ceramic Polymer and Fillers to Produce Hardystonite (Ca 2
47
48 ZnSi 2 O 7) Bioceramic Scaffolds, *J. Am. Ceram. Soc.* 99 (2016) 1960–1967.
49
50
51 doi:10.1111/jace.14213.
52
53
54 [9] M. Xu, G.M. Gratson, E.B. Duoss, R.F. Shepherd, J.A. Lewis, Biomimetic
55
56
57
58
59
60
61
62
63
64
65

1
2
3
4 silicification of 3D polyamine-rich scaffolds assembled by direct ink writing, *Soft*
5
6
7 *Matter*. 2 (2006) 205. doi:10.1039/b517278k.

8
9
10 [10] D. Therriault, S.R. White, J.A. Lewis, Chaotic mixing in three-dimensional
11
12 microvascular networks fabricated by direct-write assembly, *Nat. Mater.* 2 (2003)
13
14 265–271. doi:10.1038/nmat863.

15
16
17 [11] J.A. Lewis, J.E. Smay, J. Stuecker, J. Cesarano, Direct ink writing of three-
18
19 dimensional ceramic structures, *J. Am. Ceram. Soc.* 89 (2006) 3599–3609.
20
21 doi:10.1111/j.1551-2916.2006.01382.x.

22
23
24 [12] J.E. Smay, J.A. Lewis, *Ceramics and Composites Processing Methods*, in: N.P.
25
26 Bansal, A.R. Boccaccini (Eds.), *Ceram. Compos. Process. Methods*, Wiley,
27
28 2012: p. 596.

29
30
31 [13] V. De Graef, F. Depypere, M. Minnaert, K. Dewettinck, Chocolate yield stress as
32
33 measured by oscillatory rheology, *Food Res. Int.* 44 (2011) 2660–2665.
34
35 doi:10.1016/j.foodres.2011.05.009.

36
37
38 [14] F.J. Martínez-Vázquez, F.H. Perera, I. van der Meulen, A. Heise, A. Pajares, P.
39
40 Miranda, Impregnation of β -tricalcium phosphate robocast scaffolds by in situ
41
42 polymerization., *J. Biomed. Mater. Res. A.* 101 (2013) 3086–3096.
43
44 doi:10.1002/jbm.a.34609.

45
46
47 [15] E. Feilden, E.G.-T. Blanca, F. Giuliani, E. Saiz, L. Vandeperre, Robocasting of
48
49 structural ceramic parts with hydrogel inks, *J. Eur. Ceram. Soc.* 36 (2016) 2525–
50
51 2533. doi:10.1016/j.jeurceramsoc.2016.03.001.

52
53
54 [16] G. Girod, J.. Lamarche, A. Foissy, Adsorption of partially hydrolyzed
55
56
57
58
59
60
61
62
63
64
65

1
2
3
4
5
6
7
8
9
10
11
12
13
14
15
16
17
18
19
20
21
22
23
24
25
26
27
28
29
30
31
32
33
34
35
36
37
38
39
40
41
42
43
44
45
46
47
48
49
50
51
52
53
54
55
56
57
58
59
60
61
62
63
64
65

polyacrylamides on titanium dioxide, J. Colloid Interface Sci. 121 (1988) 265–272.

doi:10.1016/0021-9797(88)90430-4.

Figures

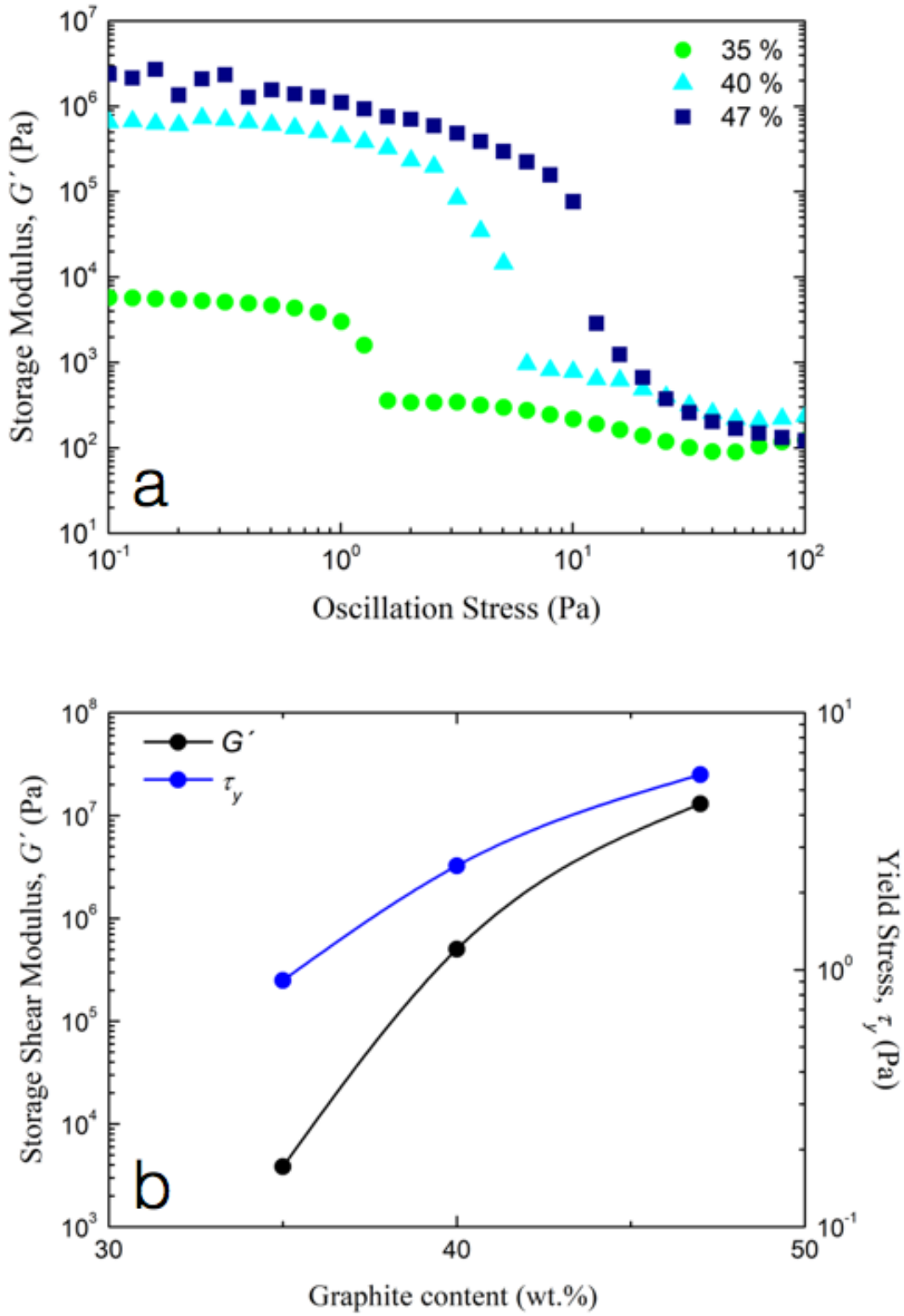


Figure 1

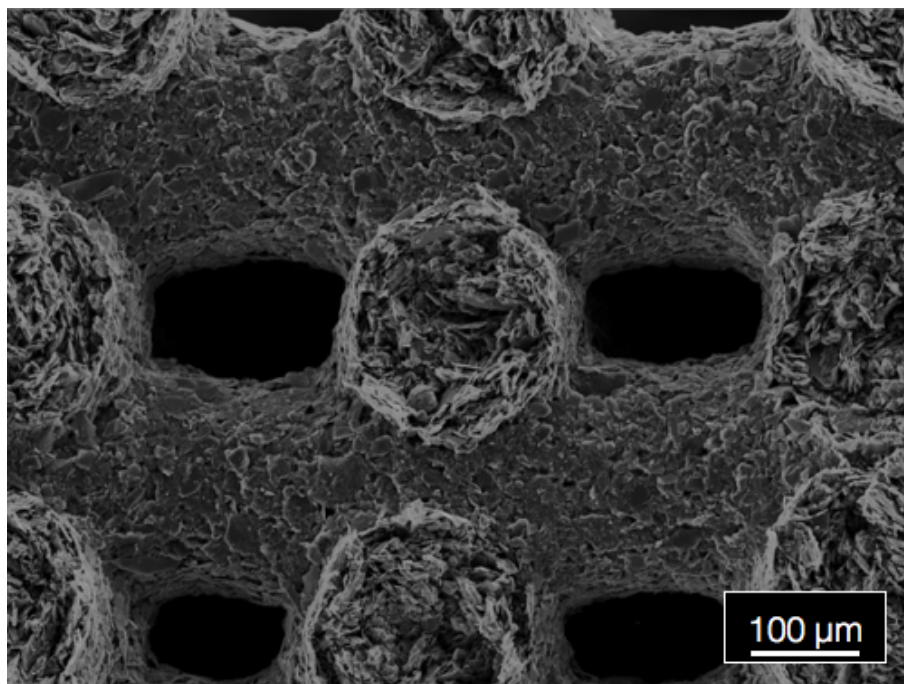


Figure 2

1
2
3
4
5
6
7
8
9
10
11
12
13
14
15
16
17
18
19
20
21
22
23
24
25
26
27
28
29
30
31
32
33
34
35
36
37
38
39
40
41
42
43
44
45
46
47
48
49
50
51
52
53
54
55
56
57
58
59
60
61
62
63
64
65

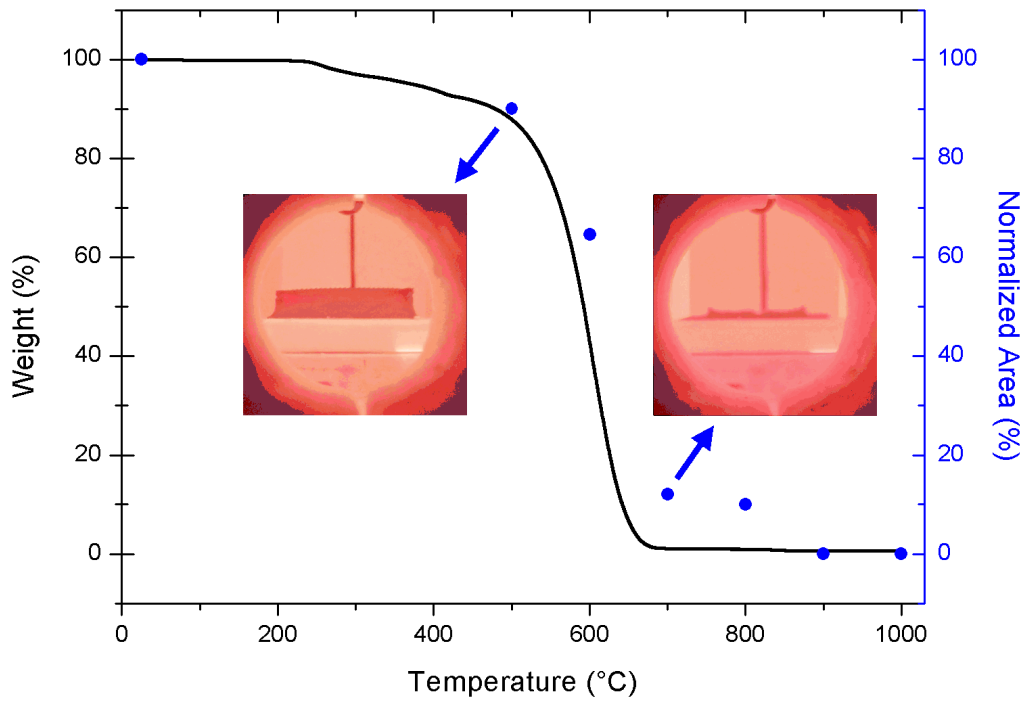


Figure 3

1
2
3
4
5
6
7
8
9
10
11
12
13
14
15
16
17
18
19
20
21
22
23
24
25
26
27
28
29
30
31
32
33
34
35
36
37
38
39
40
41
42
43
44
45
46
47
48
49
50
51
52
53
54
55
56
57
58
59
60
61
62
63
64
65

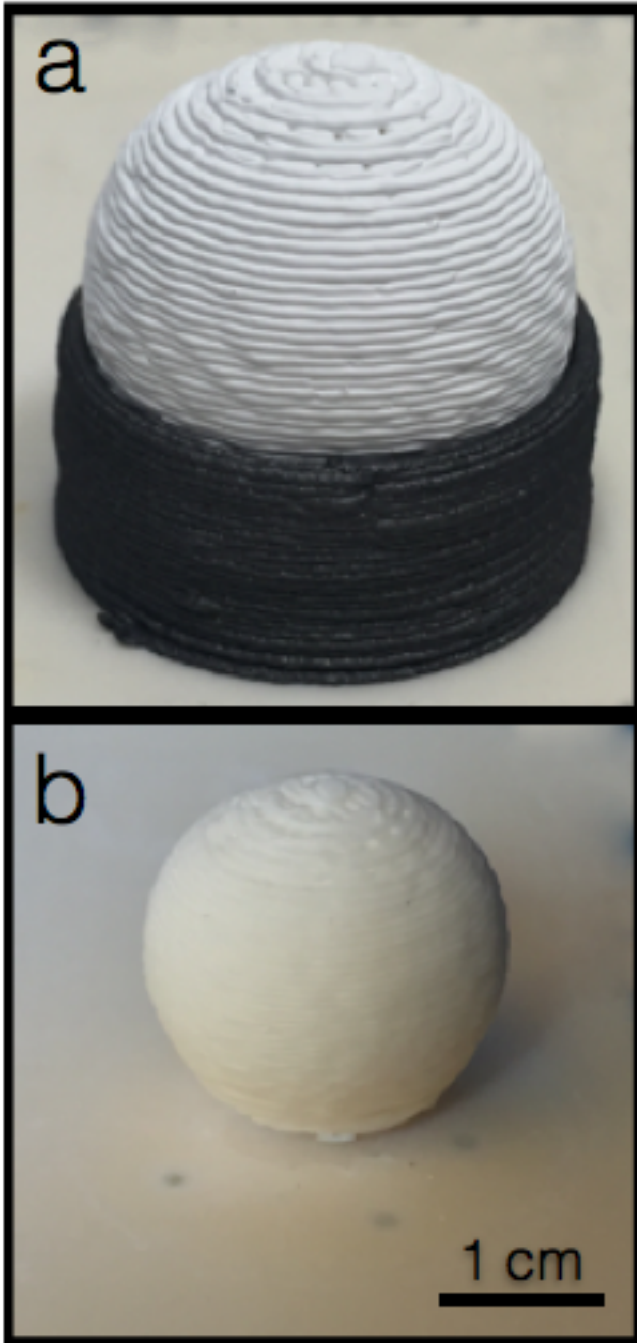


Figure 4

Figure Captions

1
2
3
4
5
6
7
8
9
10
11
12
13
14
15
16
17
18
19
20
21
22
23
24
25
26
27
28
29
30
31
32
33
34
35
36
37
38
39
40
41
42
43
44
45
46
47
48
49
50
51
52
53
54
55
56
57
58
59
60
61
62
63
64
65

Figure 1. a) Storage shear modulus, G' , as a function of oscillation stress for graphite inks with different contents (35, 40, and 47 wt.%). b) plateau storage modulus at low shear (left Y axis) and yield stress (right Y axis) of graphite inks as a function of solid content.

Figure 2. SEM image of a cross-sectional cut through a 3D graphite robocast structure fabricated using an ink with a solid-loading of 47 wt.%.

Figure 3. Weight variation from TGA measurements on a graphite ink (left Y axis) and evolution of the cross-sectional normalized area of a graphite **sample** with temperature. In situ optical images of the **sample** are provided at temperatures corresponding to the indicated points.

Figure 4. Optical images of an alumina sphere assembled by robocasting using graphite ink as a fugitive support: a) as-printed; b) after burn-out and sintering.